

## ON THE ORIGIN OF INCLUSIVE ELECTRON EVENTS IN $e^+e^-$ ANNIHILATION BETWEEN 3.6 AND 5.2 GeV

DASP Collaboration

R. BRANDELIK, W. BRAUNSCHWEIG, H.-U. MARTYN, H.G. SANDER,  
D. SCHMITZ, W. STURM and W. WALLRAFF  
*I. Physikalisches Institut der RWTH Aachen, Germany*

D. CORDS, R. FELST, R. FRIES, E. GADERMANN, H. HULTSCHIG, P. JOOS, W. KOCH,  
U. KÖTZ, H. KREHBIEL, D. KREINICK, H.L. LYNCH, W.A. McNEELY, K.C. MOFFEIT<sup>1</sup>,  
D. NOTZ, R. RÜSCH, M. SCHLIWA, B.H. WIJK and G. WOLF  
*Deutsches Elektronen-Synchrotron DESY, Hamburg, Germany*

G. GRINDHAMMER, J. LUDWIG<sup>2</sup>, K.H. MESS<sup>3</sup>, A. PETERSEN, G. POELZ, J. RINGEL,  
O. RÖMER, K. SAUERBERG and P. SCHMÜSER  
*II. Institut für Experimentalphysik der Universität Hamburg, Germany*

W. De BOER, G. BUSCHHORN, W. FUES, Ch. Von GAGERN, B. GUNDERSON,  
R. KOTTHAUS, H. LIERL and H. OBERLACK  
*Max-Planck-Institut für Physik und Astrophysik, München, Germany*

S. ORITO, T. SUDA, Y. TOTSUKA and S. YAMADA  
*Lab. of Int. Coll. on Elementary Particle Physics and Dept. of Physics, University of Tokyo, Tokyo, Japan*

Received 15 June 1977

The multiplicity distribution of inclusive electron events above 4 GeV cm energy shows two distinct classes of events: two prong no photon and high multiplicity events. If the high multiplicity events are attributed to the semi-leptonic decay of charmed particles the two prong no photon events must come from the weak decay of a different type of particle. The charged  $K$  to  $\pi$  ratio was measured for these events. The average number of charged kaons is  $0.07 \pm 0.06$  per two prong event and  $0.90 \pm 0.18$  per multiprong event. Thus the weak current responsible for the low multiplicity events has a small coupling to strange particles.

Studies of inclusive leptonic final states resulting from  $e^+e^-$  annihilation in the region of 4 GeV have shown the existence of at least one kind of new, weakly decaying particle [1, 2]. The exclusive channels seen in purely hadronic decays [3] plus the inclusive strange particle final states [4, 5] provide substantial evidence that new particles having charm are produced. Studies of leptonic states suggest that in addition to

charmed particles there is another type of particle [6, 7] having weak decays. This paper will sharpen this distinction by showing that the multiplicity of charged prongs and photons accompanying an electron in the final state forms two distinct classes. Furthermore, these two classes are distinguished by having substantially different coupling to strange particles.

The inclusive electron spectrum resulting from  $e^+e^-$  collisions at DORIS was measured using the double arm spectrometer DASP. Data were collected at cm energies between 3.6 and 5.2 GeV for a total integrated luminosity of  $6300 \text{ nb}^{-1}$ . This is nearly ten times the

<sup>1</sup> Now at SLAC.

<sup>2</sup> Now at California Institute of Technology.

<sup>3</sup> Now at CERN.

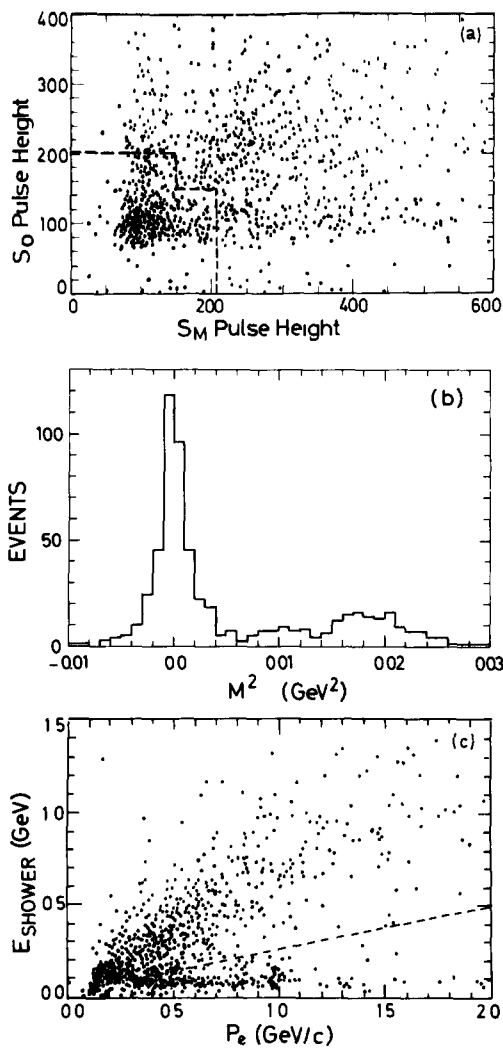


Fig. 1. Data distributions at various stages of the event selection procedure. (a) Pulse height distributions in the scintillation counters  $S_0$  and  $S_M$  in front of and behind the Čerenkov counter. The inside of the dashed curve marks the accepted region. (b) Distribution of the square of the mass as calculated for single electron candidates from the time-of-flight and momentum measurements for momenta  $< 0.35$  GeV/c. (c) Shower counter pulse heights versus momentum of the electron in the outer detector. Acceptable events with momentum  $p_e > 0.35$  GeV/c had to lie above the dashed line.

luminosity used for our previous publication [1].

A detailed discussion of the DASP detector can be found elsewhere [1, 8]. Here we describe only the features most important for this analysis. The DASP de-

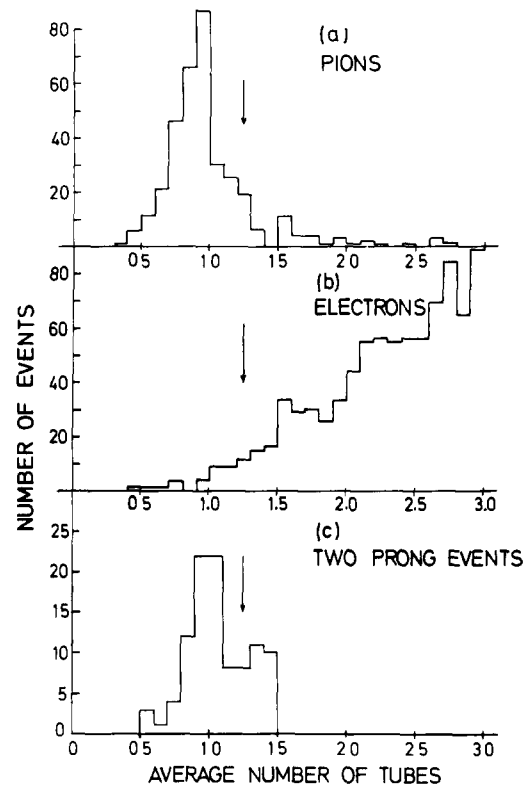


Fig. 2. Response of the inner detector to charged pions and electrons. Plotted is the average number of tubes fired per layer, corrected for angle of incidence. (a) for pions, (b) for electrons, (c) for charged tracks from two prong event before the tight nonshowering cut (see text) was made

tector consists of two identical spectrometer arms positioned symmetrically with respect to the interaction point. A charged particle emitted at the interaction point in the direction of one of the magnet arms traverses a scintillation counter  $S_0$  close to the beam pipe, two proportional chambers, a threshold Čerenkov counter, a second scintillation counter  $S_M$  and a wire spark chamber before reaching the magnet. The Čerenkov counters, which are filled with Freon 114 at atmospheric pressure ( $n = 1.0014$ ), detect electrons above 10 MeV/c, and pions above 2.8 GeV/c. Beyond the magnet the particle passes through five wire spark chambers and a wall of time-of-flight and shower counters. The shower counters are followed by iron plates interspersed with wire chambers at depths of 40 and 80 cm and a plane of scintillation counters at a depth of 70 cm of iron.

A nonmagnetic detector covering 70% of  $4\pi$  is

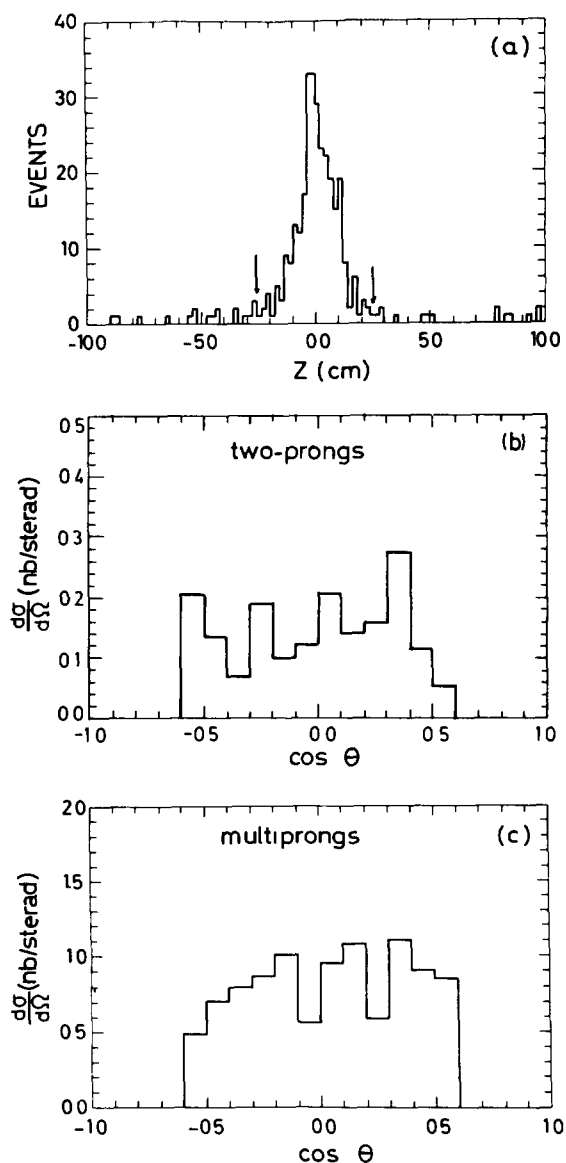


Fig. 3. (a) Distribution of the event vertex along the beam axis. Arrows indicate the region of acceptable events. (b) The electron production angular distribution for two prong events. The abscissa defines the cosine of the production angle with respect to the initial electron of the same charge (i.e. forward and backward angles are distinguished). (c) Same as (b) for multiprong events.

mounted between the two magnetic arms. A particle emitted toward this "inner detector" traverses the following elements: one of 20 scintillation counters surrounding the beam pipe, two proportional chambers

(in part of the acceptance), four modules each made of a scintillation counter hodoscope, a 5 mm thick lead converter and a tube chamber with two or three planes of proportional tubes, and finally a lead scintillation counter hodoscope 7 radiation lengths thick.

A trigger by a single charged particle requires the scintillation counters  $S_O$  and  $S_M$  in front of the magnet and a time-of-flight and a shower counter in the rear. For most of the data the magnet current was set so that electrons of momentum 0.1 GeV/c and above were accepted. The data were grouped into four intervals in cm energy: 3.60 – 3.67 GeV ( $630 \text{ nb}^{-1}$ ), 3.67 – 3.70 GeV ( $129 \text{ nb}^{-1}$ ), 3.99 – 4.52 GeV ( $3159 \text{ nb}^{-1}$ ) and 4.52 – 5.2 GeV ( $2504 \text{ nb}^{-1}$ ). The numbers in parentheses give the integrated luminosity.

The first stage of event selection defined an electron as a track which was detected by the proper Čerenkov counter and which passed through the magnet. To suppress events of electromagnetic origin an additional charged nonshowering track was required. This could be either 1) a track in a spectrometer arm identified as a hadron by time-of-flight and shower counter criteria [8] or a muon in the range telescope, or 2) a charged track in the inner detector penetrating a least three of the four scintillator/lead/proportional tube modules. The number of tubes fired per layer had to be less than 1.5 when averaged over all layers in which at least one tube fired. A correction was made for angle of incidence. A total of 1184 events satisfied these criteria. Possible sources of contamination of this sample and the measures taken to eliminate them will now be considered.

We first show that we observe events with a single electron traversing the magnet.

1. Background electrons can be produced from  $\pi^0$ 's or  $\eta$  via Dalitz decay or when a photon converts in the material in front of the Čerenkov counter. Usually the  $e^+$  and  $e^-$  travel close together, so that each deposits energy in the scintillation counters  $S_O$  and  $S_M$ . A scatter plot of the pulse heights (fig. 1a) shows a distinct cluster at  $S_O = S_M = 100$ , corresponding to the passage of a single minimum ionizing particle. There is also an accumulation of events near  $S_O = S_M = 200$  corresponding to two tracks passing through the chambers. The dotted line in fig. 1a indicates the pulse height cut applied; 83% of single electrons and  $0.8^{+0.3}_{-0.6}\%$  of double track events are accepted. The electron efficiency was determined using Bhabha events and the double track efficiency using multihadron events. After this cut 634

Table 1

Multiplicity distributions: The number of inclusive electron events are given with  $N_{\text{ch}}$  charged tracks (including the electron) and  $N_{\gamma}$  photons observed. The electron momentum is  $p_e > 0.2 \text{ GeV}/c$ .

(a) $E_{\text{cm}} = 3.99 - 4.52 \text{ GeV}$										
$N_{\text{ch}}$	2	3	4	5	6	7	8	9	10	
$N_{\gamma}$										
0	21	9	13	6	3	2				
1	6	5	9	6	5	2	1			
2	4	7	8	6	2		1			
3		2	1	2	2					
4			1	2	1	1				
5					1	1				
6			1			1				
7	1	1								

(b) $E_{\text{cm}} = 4.52 - 5.2 \text{ GeV}$										
$N_{\text{ch}}$	2	3	4	5	6	7	8	9	10	
$N_{\gamma}$										
0	16	9	9	6	1	2		1	1	
1	9	7	2	1	5	2				
2	3	1	3	3	2	2	1			
3			1	3	1	1				
4		2		1						
5		1	2	1	1		1			
6			1			1				
7			1							

events remained, of which  $17 \pm 5$  events are estimated to be background from  $\pi^0$  or  $\eta$ .

2. Of the charged hadrons  $0.7 \pm 0.2\%$  produce knock-on electrons or scintillate and make a signal in the Čerenkov counter. Therefore an independent electron identification was required. For tracks of momentum  $p < 0.35 \text{ GeV}/c$  the velocity measured by time-of-flight was required to be above  $0.967 c$ . Fig. 1b shows the mass spectrum calculated from the measured momentum and time-of-flight. Electrons of momentum  $p > 0.35 \text{ GeV}/c$  were required to deposit an energy of at least  $0.25 p$  in the shower counters (fig. 1c). In total 483 events survived this cut of which 9 events could be background from misidentified hadrons.

3. Each candidate was inspected by physicists and the number of charged tracks (prongs) and photons was determined. In this scan events of obvious electromagnetic origin, e.g. Bhabha events where one electron

showered in the beam pipe, were rejected.

4. Electromagnetic background contaminates mostly events with two charged particles plus any number of photons (two prongs). For these the first stage criteria for the nonshowering track were tightened. It had to 1) penetrate all four modules (this imposed a minimum momentum cut of  $0.1 \text{ GeV}/c$  on pions); 2) activate at least one proportional tube in each unit; 3) activate 7 of the 9 (9 of 12) tube planes in the side (top/bottom) parts of the inner detector; and 4) activate an average of fewer than 1.25 tubes per plane hit (corrected for incidence angle).

The response of the inner detector proportional tubes to pion tracks was studied using  $e^+e^- \rightarrow \psi' \rightarrow \text{J}/\psi \pi^+\pi^- \rightarrow e^+e^- \pi^+\pi^-$  events and  $\text{J}/\psi \rightarrow \pi^0\rho^0 \rightarrow \gamma\gamma\pi^+\pi^-$  events as sources of low and high energy pions, respectively. The response to electron tracks was studied using wide angle bremsstrahlung events  $e^+e^- \rightarrow e^+e^-\gamma$ . Fig. 2a-c show the average number of tubes fired per layer (corrected for incidence angle) for pions, electrons and the nonshowering tracks from two-prong event candidates before the tight cut was made. We find that 95% of all pions, but fewer than 5% of electrons satisfy the tight criteria. We estimate that for fewer than 5% of the two prong events can the "nonshowering" track in fact be an electron.

We now show that the surviving electron events have no trivial explanation.

1. The number of events due to inelastic electron scattering on the residual gas in the storage ring was determined from the distribution of the vertex position  $z$  along the beam (see fig. 3a). We required  $|z| < 2.5 \text{ cm}$ . From the region  $|z| > 3 \text{ cm}$  we estimate a  $2.5 \pm 0.6\%$  beam gas contamination.

2. The contribution from Compton scattering of a photon on an electron in the material in front of the Čerenkov counter was estimated to be less than 0.1 events. Calculation were made to estimate the number of events from semileptonic decays of pions and kaons (0.8 events) and of leptonic decays of vector mesons ( $< 0.1$  events).

3. Of the possible two photon exchange processes,  $e^+e^- \rightarrow e^+e^- + \text{hadrons}$  and  $e^+e^- \rightarrow e^+e^-\mu^+\mu^-$ , the latter represents the larger background. Our range of polar angle acceptance for the electron  $|\cos \theta| < 0.6$  limits the contribution to 3 events for two prongs and less than 0.5 events for multiprongs [9]. The absence of any appreciable contribution from the  $2\gamma$  processes is

Table 2

Number of  $e\pi^\pm X$  and  $eK^\pm X$  events with  $\pi$  or  $K$  momentum above 0.4 GeV/c as a function of the total number of charged particles observed,  $N_{ch}$ ,  $E_{cm}$  is the cm energy,  $R_{K\pi}$  is the ratio of charged  $K$  to  $\pi$  production for these electron events corrected for decay losses and background contributions

$E_{cm}$	$N_{ch} = 2$			$N_{ch} \geq 3$		
	$N_{e\pi^\pm X}$	$N_{eK^\pm X}$	$R_{K\pi}$	$N_{e\pi^\pm X}$	$N_{eK^\pm X}$	$R_{K\pi}$
3.99 – 4.52	24	1	0.06 ± 0.06	219	23	0.25 ± 0.06
4.52 – 5.2	16	1	0.14 ± 0.14	136	13	0.23 ± 0.07

verified by the polar angular distributions of the electron shown in figs. 3b, c for accepted candidates. The angular distribution from the  $2\gamma$  processes is sharply peaked forward while the measured distributions are flat.

The background estimates given above can be tested experimentally using data collected below charm threshold. By studying  $\psi'$  decays one learns how often a purely hadronic event appears to contain a single electron. At the  $\psi'$  resonance 0.63 times as many inclusive hadron events were recorded as in the data above 4 GeV. These yielded zero two prong candidates and 21 multiprong candidates after obvious cascade decays were eliminated. Data in the nonresonant region below charm threshold measure background from electromagnetic and hadronic events. The data at 3.6 GeV resulted in 5 candidates two of which were two prong events. Combining these numbers yields a measured background of  $20 \pm 14\%$  for the two prong class in agreement with the estimated value of  $11.5 \pm 3.5\%$ . The latter value is used in the analysis. The measured background for multiprong events is  $17 \pm 4\%$  compared to the computed value of  $15 \pm 5\%$ .

After all cuts 66 two prong and 190 multiprong events survived. In the following analysis we retain electron momenta above 0.2 GeV/c, leaving 60 and 182 events in these categories, respectively. They were classified according to the observed number of charged particles  $N_{ch}$  (including the electron) and photon  $N_\gamma$ . The results, divided into the energy intervals 3.99 – 4.52 and 4.52 – 5.2 GeV, are listed in table 1. In order to arrive at the true multiplicity distribution one must correct for particle detection efficiencies. A Monte Carlo study yielded a charged particle detection efficiency of  $0.73 \pm 0.05$  and a photon efficiency of  $0.70 \pm 0.05$ . Most of the 242 events have high multiplicities. However, the single most populous channel has two charged tracks and no photons. It is impossible

to understand this channel as leak through from higher multiplicity events. Using the observed multiplicity distribution we estimate that only  $3.6 \pm 0.8$  of the 21 events at 3.99 – 4.52 GeV and  $3.1 \pm 0.8$  of the 16 events at 4.52 – 5.2 GeV come from higher multiplicities. Subtracting these events and the background estimated above leaves  $26 \pm 7$  two prong no photon events in the combined energy regions. We conclude there exists a genuine two-prong no photon class of events. The corrected average charge and photon multiplicities, excluding the two prong no photon events are  $(N_{ch}, N_\gamma)_{corr} = (5.5 \pm 0.3, 1.9 \pm 0.3)$  and  $(5.7 \pm 0.3, 1.8 \pm 0.3)$  for the two energy intervals, respectively. The errors are statistical only.

In our previous paper we concluded that the high multiplicity events come from the weak decays of a new type of hadron. There is now little doubt that most of these events are weak decays of charmed hadrons. We now investigate whether charm production can also explain the two prong no photon events. These events contain one electron, one nonshowering charged track ( $T^\pm$ , which could be  $\pi$ ,  $K$ ,  $p$  or  $\mu$ ) and any number of invisible neutral particles ( $N$ , which could be  $\nu$ ,  $K_L^0$  or  $n$ , but not  $\gamma$ ). Associated charmed hadron production can yield such events in three ways: 1) Charged charmed hadrons are produced, one decaying to  $e$  and invisible particles, the other to  $T^\pm$  and invisible particles, plus possible invisibles produced directly. 2) Neutral charmed hadrons are produced, one decaying to  $e$  and  $T^\pm$  plus invisible particles, the other decaying to invisibles. 3) A charged charmed hadron yields the  $e$ , a neutral charmed hadron decays invisibly and  $T$  is produced directly.

We have considered such production modes c.f. below, and we find that less than 12% of the two prong zero photon events have such sources: Events resulting from charmed baryon production are estimated to be less than 4% by setting upper bounds on  $\bar{p}$  or  $\bar{n}$  production.

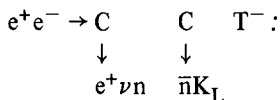
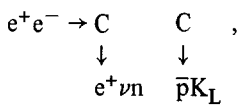
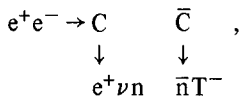
(The detection efficiency for  $\bar{n}$  is similar to the photon detection efficiency in our detector.) Charmed meson production is estimated to contribute less than 8% to the two prong zero photon events by the detailed arguments given below. We therefore conclude that these events cannot be explained by charm, but rather some other new particles must be responsible for them. We now consider such production modes in detail, making use of three properties of charmed hadrons;

a) Charmed particles decay to particles which are eigenstates of strangeness, e.g.  $D^0$  decays to  $K^0$  but not into pure  $K_L^0$  or  $K_S^0$ .

b) Charmed particle decays follow the GIM mechanism [10].

c) The lowest charmed baryon state is the  $\Lambda_c(2260)$  [11].

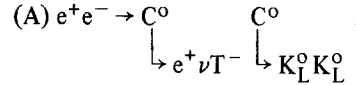
We dispense first with charmed baryon production. The possible charmed baryon processes which can contribute are (omitting the charge conjugate reactions):



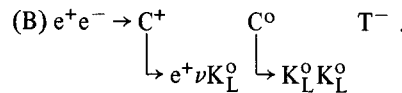
We use the symbol C to refer generically to charmed hadrons. In our detector an antineutron looks like one or several high energy photons. Due to the large amount of sensitive material ( $70 \text{ gm/cm}^2$ ), the detection efficiency for  $\bar{n}$  is essentially the same as for a photon. This calculation has been checked by studying  $J/\psi \rightarrow \pi^- p \bar{n}$  events. A  $\bar{p}$ , if there, must be the "nonshowering" track T. But fewer than 10% of  $\bar{p}$  satisfy the tight criteria for a single nonshowering track. Furthermore, if charmed baryon production were important, it could contribute only above  $\Lambda_c(2260)$  threshold, i.e. above 4.52 GeV. However, no significant change is seen in the fraction of two prong no photon events below and above the threshold for charmed baryon production (see table 1). We now assume that charmed baryon production on the average leads to an equal number of  $\bar{n}$  and  $\bar{p}$ . With the conservative assumption that the total

measured  $\bar{p}$  yield [8] results from charmed baryon production, observing that the particular decay  $C \rightarrow e\nu n$  involved in all three modes is GIM suppressed by a factor of 0.05 and using the  $\bar{p}$  and  $\bar{n}$  detection efficiencies we find that less than 4% of the two prong no photon events can be attributed to charmed baryon production.

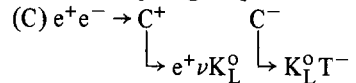
We now consider the three possible charmed meson production processes which could make two prong no photon events<sup>+1</sup>.



The decay  $C^0 \rightarrow K^0 \bar{K}^0$  is GIM suppressed by a factor  $\sin^2\theta_c = 0.05$ . Favored decays, e.g.  $C^0 \rightarrow K^+\pi^-$ , produce additional easily detected charged particles or photons. The observed distribution of event topologies limits this production mode to less than 2% of the interesting events.



The same arguments apply to this reaction. The combined contribution from channels A and B is less than 2% of the two prong no photon events.



Because charmed mesons decay to eigenstates of strangeness,  $K_S^0$  must appear as frequently as  $K_L^0$ . A  $K_S^0$  decays into visible pions or photons, feeding other topologies. A fit to the topology distribution using the particle detection efficiencies shows that  $0 \pm 6\%$  of the two prong no photon events are due to this reaction. This number includes also a part of the possible contribution from channels A and B.

A crucial difference between the GIM current and the normal Cabibbo current is the different coupling strength to strangeness. This coupling was investigated by studying events having an identified charged hadron ( $\pi$ , K or  $\bar{p}$ ) in one spectrometer arm [8], an electron in the inner detector, and possible other charged particles or photons. The electron was identified by demanding a showering charged track in the inner detector (see discussion above and fig. 2). The efficiency for an electron in the geometrical acceptance of the inner detec-

<sup>+1</sup> The leptonic decay modes  $C \rightarrow e\nu$  and  $C \rightarrow \mu\nu$  can be neglected as shown by the electrom momentum spectrum [12].

tor to pass the electron cuts was a smooth function of momentum: 50% at 0.4 GeV/c, 80% at 0.7 GeV/c and over 90% above 1 GeV/c. No events were found in the data taken at 3.6 GeV. The number of events observed at higher energies are given in table 2. The estimated background is small. No  $e\bar{p}X$  events were found. After correcting for decay losses and background contributions the ratio of charged K to  $\pi$  production  $R_{K\pi}$  was determined for particle momenta above 0.4 GeV/c. The values are given in table 2. From the observed K to  $\pi$  ratio for multiprong events and the measured charge multiplicity we conclude that each event contains on the average  $0.90 \pm 0.18$  charged kaons per event. The two prong events, however, contain an average of only  $0.07 \pm 0.06$  kaons per event. This shows that for charmed particles (i.e. high multiplicity) the weak current couples strongly to strangeness in accord with the GIM mechanism. On the contrary, for the two prong class the weak current has a small coupling to strange particles, consistent with the normal Cabibbo current.

In summary we have observed 242 electron inclusive events for cm energies between 3.99 and 5.2 GeV with an average background of 14%. The multiplicity distribution of charged tracks and photons show two types of events, those with several charged particles and photons and those with two charged particles and no photons. The relative frequency of two prong no photon events and multiprong events cannot be understood by assuming that charm particle production accounts for all events. We conclude that we are observing two distinct processes, production and weak decay of charmed particles (multi-prong-events) as well as production and weak decay of a different type of particle (two prong events). We also conclude from the measured charged K to  $\pi$  ratio for low and high charge multiplicities that the weak current responsible for the low multiplicity events has a small coupling to strange particles consistent with the familiar Cabibbo current, while the high multiplicity events have a much stronger coupling to strange particles in accord with the GIM mechanism.

We are grateful to Dr. T. Walsh for numerous discussions. We are indebted to all the engineers and technicians of the collaborating institutions who have participated in the construction and maintenance of DASP. The invaluable cooperation of the technical support groups and the computer center at DESY is gratefully acknowledged. We are indebted to the DORIS machine group for their excellent support during the experiment. The non-DESY members of the collaboration thank the DESY directorate for their kind hospitality. S. Yamada wishes to thank the Mitsubishi Foundation and Yoshida Foundation for Science and Technology for partial financial support.

## References

- [1] DASP Collaboration, W Braunschweig et al., Phys. Lett 63B (1976) 417.
- [2] See also Pluto Collaboration, J. Burmester et al., Phys Lett. 66B (1976) 395.
- [3] G Goldhaber et al., Phys Rev Lett. 37 (1976) 255, I Peruzzi et al., Phys. Rev. Lett. 37 (1976) 569, J.E. Wiss et al., Phys. Rev. Lett. 37 (1976) 1531
- [4] DASP Collaboration, R Brandelik et al., Phys Lett. 67B (1977) 363
- [5] Pluto Collaboration, J. Burmester et al., Phys Lett. 67B (1977) 367
- [6] M. Perl et al., Phys Rev Lett 35 (1975) 1489, 63B (1976) 466.
- [7] Pluto Collaboration, J. Burmester et al., Phys. Lett. 68B (1977) 297, 301
- [8] DASP Collaboration, R Brandelik et al., Phys. Lett. 67B (1977) 358
- [9] For a similar calculation see e.g. J. Parisi, Intern. Colloq. on Photon-photon collisions in electron-positron storage rings, Paris, 1973.
- [10] S.L. Glashow, J Iliopoulos and L Maiani, Phys Rev. D2 (1970) 1285.
- [11] E.G. Gazzoli et al., Phys Rev Lett. 34 (1975) 1125, B. Knapp et al., Phys. Rev. Lett. 37 (1976) 882
- [12] DASP Collaboration, R. Brandelik et al., DESY Report, 1977.